ELSEVIER

Biophysical Chemistry 105 (2003) 323–338

Biophysical Chemistry

www.elsevier.com/locate/bpc

Hydration of krypton and consideration of clathrate models of hydrophobic effects from the perspective of quasi-chemical theory

Henry S. Ashbaugh[a], D. Asthagiri[a], Lawrence R. Pratt[a,*], Susan B. Rempe[b]

[a]*Theoretical Division, Los Alamos National Laboratory, Los Alamos, NM 87545, USA*
[b]*Sandia National Laboratories, Albuquerque, NM 87185, USA*

Received 16 October 2002; received in revised form 7 November 2002; accepted 7 November 2002

Abstract

Ab initio molecular dynamics (AIMD) results on a krypton–water liquid solution are presented and compared to recent XAFS results for the radial hydration structure for a Kr atom in liquid water solution. Though these AIMD calculations have important limitations of scale, the comparisons with the liquid solution results are satisfactory and significantly different from the radial distributions extracted from the data on the solid Kr/H_2O clathrate hydrate phase. The calculations also produce the coordination number distribution that can be examined for metastable coordination structures suggesting possibilities for clathrate-like organization; none are seen in these results. Clathrate pictures of hydrophobic hydration are discussed, as is the quasi-chemical theory that should provide a basis for clathrate pictures. Outer shell contributions are discussed and estimated; they are positive and larger than the positive experimental hydration free energy of Kr(aq), implying that inner shell contributions must be negative and of comparable size. Clathrate-like inner shell hydration structures on a Kr atom solute are obtained for some, but not all, of the coordination number cases observed in the simulation. The structures found have a delicate stability. Inner shell coordination structures extracted from the simulation of the liquid, and then subjected to quantum chemical optimization, always decomposed. Interactions with the outer shell material are decisive in stabilizing coordination structures observed in liquid solution and in clathrate phases. The primitive quasi-chemical estimate that uses a dielectric model for the influence of the outer shell material on the inner shell equilibria gives a contribution to hydration free energy that is positive and larger than the experimental hydration free energy. The 'what are we to tell students' question about hydrophobic hydration, often answered with structural clathrate pictures, is then considered; we propose an alternative answer that is consistent with successful molecular theories of hydrophobic effects and based upon distinctive observable properties of liquid water. Considerations of parsimony, for instance Ockham's razor, then suggest that additional structural hypotheses in response to 'what are we to tell students' are not required at this stage.

Keywords: Hydrophobic hydration; Clathrate hydrate; Ab initio molecular dynamics; Quasi-chemical theory; Scaled particle theory; Krypton

*Corresponding author.

0301-4622/03/$ - see front matter © 2003 Elsevier Science B.V. All rights reserved.
doi:10.1016/S0301-4622(03)00084-X

1. Introduction

Kauzmann's analysis [1] established the topic of hydrophobic effects as relevant to the structure, stability, and function of soluble proteins. Reminiscences on protein research of that period emphasize that the concept of hydrophobic stabilization of globular proteins was non-trivial [2]. Decades have passed, and the language of hydrophobic effects has become common. It is therefore astonishing to note that consensus on a molecular scale conceptualization of hydrophobic effects, and on molecular theories, has not been obtained. For a recent example, see Lazaridis [3]. In the present setting of competing ideas, theories, and selected results, it is not uncommon to hear from biophysical chemists, 'What are we to tell students?' Of course, one response is to question what we tell ourselves.

In addressing the most primitive hydrophobic effects, molecular theory has achieved some surprising steps recently. A compelling molecular theory for primitive hydrophobic effects is now available [4], though a variety of more complex cases have not been similarly resolved [5]. Still, the recent theoretical advance means that we can scrutinize conflicting theories more seriously and begin to build a more objective answer to the 'what are we to tell students' question.

The recent XAFS studies of the hydration of Kr in liquid water and in a comparable solid Kr/H_2O clathrate phase [6] seem particularly helpful to the task of consolidation of molecular theories of primitive hydrophobic effects. These experiments were directed toward characterization of the iceberg pictorial interpretations and conclusions of Frank and Evans [7] that were supported in part by the known structures of solid clathrate hydrates.

In the panoply of *pictures* of hydrophobic phenomena, clathrate models are especially appropriate as initial targets for modern scrutiny: it has been discovered recently how these structural models might be developed logically as a basis for molecular theory of hydrophobic effects [8,9]. Those approaches are *quasi-chemical* theories. They hold promise for higher molecular resolution, and particularly for treating *context hydrophobicity* in which proximal hydrophilic groups affect the hydration of hydrophobic moieties.

A drawback that can be foreseen for quasi-chemical theories is one that is common to computational chemistry: several competing contributions must be evaluated at an appropriate accuracy and assembled. The net hydration free energy of Kr(aq) is an order of magnitude smaller than several of the primitive contributions to it. Every little thing counts in the assembled results and experience in evaluating the various required contributions is thin. The chemically simple case of Kr(aq) is an appropriate starting point because the various contributions that must be evaluated seem to be in hand. Nevertheless, detailed computational determination of the hydration free energy of Kr(aq) is not sought in the present effort, which instead takes the goals of testing clathrate pictures of hydrophobic hydration and of scoping molecularly detailed quasi-chemical theories.

The plan for this paper is as follows. In the next section we give some background on clathrate models of hydrophobic hydration. After that, we discuss the quasi-chemical theory in order to explain the coordination number distribution that is the principal target of the following ab initio molecular dynamics (AIMD) calculations. AIMD results for the hydration of Kr(aq) are then compared with results from the XAFS experiments. To guide quasi-chemical descriptions of these phases, we then estimate the inner and outer shell contributions required for the most primitive approximations. The final sections discuss 'what are we to tell students' and identify conclusions.

Though AIMD calculations might seem to be excessive for this chemically simple problem, this approach is available and the results are not limited by assumptions of non-cooperativity of the interactions. Modern work [10–12] on hydrophobic hydration has suggested that attractive interactions between solute and solvent water might play a role less trivial than assumed by conventional van der Waals theories [13]. This point is consistent with the fact that clathrate phases involving inert gases as light as Ne are more exotic and are to be sought at relatively higher pressures than similar phases involving heavier inert gases [14–17].

The present work is centered on the physical–chemical basics of a foundational concept of molecular structural biology. We hope this focus follows the example provided by Kauzmann's wide-ranging considerations of molecular science, including topics of water and aqueous solutions [18] and molecular biophysical chemistry.

2. Clathrate model background

The status of clathrate pictures of hydrophobicity is reflected in the current literature; for example, see Cheng and Rossky [19]. 'Conventional views hold that the hydration shell of small hydrophobic solutes is clathrate-like, characterized by local cage-like hydrogen-bonding structures and a distinct loss in entropy.' An admirably clear and appropriately circumspect early consideration of clathrate models for solutions of hydrophobic gases in liquid water was given by Glew [20]. The data available at that time suggested '…that the nature of the water solvent surrounding weakly interacting aqueous solutes should be likened geometrically to those coordination polyhedra experimentally observed in the solid gas-hydrates.' Still, 'in no sense is it considered that the water molecules adjacent to the solute are permanently immobilized or rigid as in solid structures…' [20]. The more recent discussion of Dill [21] explains conventional views of hydrophobic hydration '…that the organization of water molecules in the first shell surrounding the solute is like an 'iceberg', a clathrate, or a 'flickering cluster.'' It may be disconcerting that a series of non-equivalent descriptors are used for the same phenomenon. This fact reflects the imprecision of these conceptualizations, and we will not distinguish them further. Another much earlier expression of such a physical view can be found in Klotz [22]; at the same time a clathrate model of liquid water *without* solutes was proposed by Pauling [23]. The review in Southall et al. [24] discussed again Kauzmann's consideration [1] of clathrate models of hydrophobic hydration, which argued that the degree of ordering suggested by measured hydration entropy changes upon dissolution was too small to be conceived as crystalline ordering. Concluding, Kauzmann [1] stated: 'There is no justification for using the iceberg concept as a basis for the hypothesis that protein molecules are surrounded and stabilized by regions of ordered water molecules.'

On the solution structure side of this issue, Head-Gordon [25] examined the question of whether the structure of liquid water near hydrophobic inert gas molecules was clathrate-like by exploiting computer simulation to compute the numbers of H-bonded pentagons present near those solutes compared to bulk regions of liquids. The idea was that pentagonal bonding structures are evident in clathrate crystals so pentagons might be a suitable diagnostic of clathrate-like structures in liquid solutions. Some enhancement of the populations of pentagons was observed in the first hydration shell of model CH_4 solute in liquid water, but the conclusions were ultimately mixed and included that 'it is important to emphasize that no direct connection between structure and thermodynamics is made—i.e. through a formal statistical mechanical theory.'

On the crystal side of this issue, clathrate phases with impressively complex guests have been discovered [26,27]. But it can happen that though the water molecules are ordered, the structure of the guest molecule is disordered. That is opposite to the case sought in protein crystallography. Earlier [28] analysis of crambin crystals had identified a cluster of pentagonal rings of water molecules at the surface of that protein. Those rings are H-bonded to the protein and crystal packing effects are involved in principle. It has been challenged [29] whether pentagonal H-bond structures are general features of hydration of soluble proteins. Furthermore, as noted in the statement above, the thermodynamic significance of such structures hasn't been established. The XAFS results of Bowron et al. [6], which are a motivation for this work, were directed toward an experimental test of this clathrate concept. Conditions were chosen to permit formation of a Kr clathrate from the liquid solution in the sample cell. Temperatures ranged from an initial 5 °C to −5 °C with pressures of approximately 110 bar. Results taken before and after the transition permitted comparison of the radial distribution of water oxygen atoms conditional on a Kr atom. Those inferred

radial distributions for the liquid solution and the clathrate phase were *qualitatively* different, as is discussed further below. This difference would be a serious problem for a literal interpretation in terms of a clathrate model of hydrophobicity. A reasonable correspondence of radial solvent density certainly should be a fundamental requirement of a successful clathrate model, and it is a requirement that has received less attention than orientational distributions.

Molecular-scale simulation of aqueous solutions of hydrophobic solutes and of systems that form clathrates of common interest has been pursued many times over several decades. Much of that work on solutions is refered to in Pratt [4]. An early example of molecular simulation of a methane clathrate is described in Tse et al. [30]; a comparable, more recent example can be found in Forrisdahl et al. [31] and a comprehensive review is given by Sloan [17]. Conclusions from that body of work are consistent with the results of the XAFS experiments discussed above. The radial layering of oxygen density conditional on the guest is much weaker in the solution case. Results from studies of liquid solutions yield a modest maximum value of oxygen radial distribution, typically slightly larger than 2, and with a weak minimum that provides little physical distinction between first and second hydration shells. In contrast, the maximum values of g_{co} in the methane clathrate calculations are greater than 4 with an unambiguous physical definition of the first hydration shell. The important work of Owicki and Scheraga [32] compared the radial distributions of oxygen atoms neighboring a methane solute in liquid solution to an ideal clathrate possibility. In that case, the mean inner shell occupancy was approximately 23 and the correspondence with a clathrate case seemed closest for the 24 vertex cage [17], larger than the smaller 20 vertex possibility presented by known clathrate crystals. The radial distribution was noted to be relatively diffuse in the solution case.

Distributions of orientational angles are often presented in solution simulations and sometimes compared explicitly to ideal results for clathrate crystal geometries [33]. This question of the connection between angle distributions and solution phase hydrophobicities was addressed by an information theory analysis that arranged to include systematically 2, 3,…, *n*-body solvent correlations in thermodynamic predictions of solution phase hydrophobic hydration free energies. It was a surprise that inclusion of just $n=2$ and 3-body correlations *deteriorated* the thermodynamic predictions obtained when only $n=2$-body correlations were used [4,34]. That work suggested that an exclusive focus on distributions of angles, which are obtained from 3-point distributions, can be problematic for drawing conclusions about clathrate models of hydrophobicity.

It is helpful to keep in mind the observation discussed by Friedman and Krishnan [35]: The sum of the solvation entropies of K^+ and Cl^- in water is approximately the same as twice the solvation entropy of Ar(aq), though the case of methanol as solvent was different. These hydration entropies are negative so solvent ordering is suggested. But the specific molecular ordering of near neighbor water molecules is expected to be qualitatively different in each of these cases. So there is no simple, unique inference of molecular structuring available from the measured hydration entropy; furthermore, the observed entropies generally do not imply that H-bonding interactions among water molecules are not substantially influenced by the solute.

Still, clathrate pictorial interpretations are widely assumed. Sloan [17] notes that '…the water scientific community refers to short-lived cavities (not unit crystals sI, sII or sH) as clathrate-like structures in water'. Indeed, it is common to describe the liquid solution results as 'clathrate-like' without scrutiny of likeness or unlikeness to specific clathrate possibilities.

3. Perspective from quasi-chemical theory

Quasi-chemical theories are built upon a distinction between defined inner and outer shell regions [9,36]. The intention is to define an inner shell that can be studied at molecular resolution using tools of modern computational chemistry. For the outer shell region, in contrast, genuine statistical mechanics cannot be avoided, but it ought to be simpler because complicated chemical interactions are not a direct concern there. The inner shell is

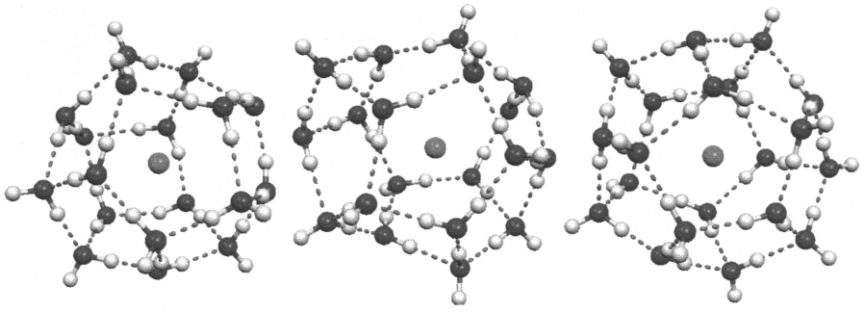

Fig. 1. Structures for $Kr[H_2O]_n$. H-bonds between the water molecules are depicted by broken lines. From left to right, the structures have 18, 19 and 20 water molecules, respectively. Oxygen atoms are red, hydrogen atoms are blue, and the krypton atom is blue.

defined geometrically [8] by specification of an indicator function $b(\mathbf{j})$ that is one (1) when solution molecule **j** occupies the intended inner shell and zero (0) otherwise. Fig. 1 shows candidates for inner shell complexes $Kr(H_2O)_n$ and suggests how this approach might apply to build statistical thermodynamic models starting from 'clathrate-like' concepts.

With the inner shell defined, the interaction contribution to the chemical potential of the Kr solute can be expressed as [8,9]

$$\beta\mu^{ex}_{Kr(aq)} = -\ln\left(1+\sum_{m\geq 1} K_m \rho^m_{H_2O}\right) - \ln\left\langle\left\langle e^{-\beta\Delta U_{Kr}}\prod_j (1-b(\mathbf{j}))\right\rangle\right\rangle_0 \quad (1)$$

where $\beta^{-1}=kT$, with T the temperature and k the Boltzmann constant. This excess chemical potential is partitioned into an inner shell contribution [the first term on the right of Eq. (1)] and an outer shell contribution (the remainder). The inner shell contribution is associated with equilibrium of chemical equations

$$Kr + nH_2O \rightleftharpoons Kr(H_2O)_n \quad (2)$$

for the in situ formation of inner shell complexes, as in Fig. 1, in situ. The coefficients K_m are equilibrium ratios for these equations.

The coefficients K_m might be obtained by observations of the population of Kr atoms coordinated to m water molecules, $m=0,1,\ldots$ This directs attention to the probability that a distinguished Kr atom has m inner shell water molecule ligands. Those fractions will be denoted by x_m and are given by

$$x_m = \frac{K_m \rho^m_{H_2O}}{1+\sum_{n\geq 1} K_n \rho^n_{H_2O}} \quad (3)$$

The probabilities x_m are physical observables that could be obtained, for example, from a simulation. Our first goal is to investigate these x_m values to see whether they give any suggestion of coordination species present in corresponding known clathrate hydrates. We note these distributions were conventionally considered in historical computer simulations for these problems; they were then referred to as 'quasi-component' distributions [10]. This discussion attempts to situate these distributions in helpful statistical thermodynamic theories.

The natural initial implementation of these quasi-chemical ideas, particularly to ion hydration, has been to treat effects of material external to the cluster by an approximation

$$K_m \approx \exp\left[-\beta(\mu^{ex}_{Kr(H_2O)_m} - m\mu^{ex}_{H_2O})\right] K_m{}^{(0)} \quad (4)$$

where $K^{(0)}_m$ is the equilibrium ratio for Eq. (2) in a dilute gas. This approach will be used in the results below, and the required hydration free energies are obtained standardly from a dielectric continuum model [37] and includes a contribution from the outer shell term corresponding to the bare ion.

Recently, it has been indicated in Paulaitis and Pratt [9] how these inner and outer shell contributions can be naturally recombined after the most natural primitive approximations. In that sense, it is not necessary to consider these two terms separately. That development leads further to a revised approximation scheme in which $K_m \approx \gamma^m K_m^{(0)}$, with γ a Lagrange multiplier that plays the same role here as an activity coefficient. Further, $-kT\ln\gamma$ can also be seen as an effective external field operating on each ligand molecule, analogous to the prefactor of $K_m^{(0)}$ in Eq. (4), This leads finally to the concept of a self-consistent field treatment of quasi-chemical approximations [38].

4. Ab initio molecular dynamics for Kr(aq) and comparison with XAFS results

The system simulated by AIMD consisted of one Kr atom surrounded by 32 water molecules in a cubic box with sides of length 9.87 Å and periodic boundary conditions. An initial structure was obtained utilizing results from an earlier study of Li^+(aq) [39,40]. A Kr atom was substituted for the Li^+ ion in a configuration from that calculation, the full system was then optimized in a much larger cell and replaced in the original simulation cube. Optimization of configurations drawn from the subsequent molecular dynamics trajectory and variations of total optimized energies with the simulation cell size suggests that this system is at a realistically low pressure. A more precise estimate of the pressure was not possible in the present effort.

The calculations, based upon an electron density functional description [41] of the electronic structure and interatomic forces, were carried out on the Kr(aq) system utilizing the VASP program [42,43]. The ions were represented by ultrasoft pseudopotentials [44,45], in the local density approximation for Kr and in the gradient-corrected approximation for O and H, and a kinetic energy cut-off of 29.10 Ry defined the plane wave basis expansions of the valence electronic wave functions. The valence electrons consisted of eight (8) electrons for Kr (4s and 4p), six (6) electrons for O (2s and 2p), and one (1) electron for H (1s).

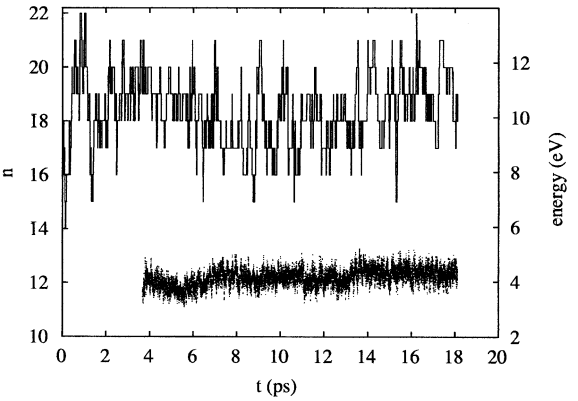

Fig. 2. Oxygen coordination of the Kr atom as a function of time (upper trace and left axis). The total kinetic energy of the atomic motion shown in the lower trace demonstrates the stability of the temperature state.

The equations of motion were integrated in time steps of 1 fs with a thermostat set at 300 K during the first 4 ps of simulation time. The thermostat was then abandoned; the temperature rose and settled at 341 ± 24 K (see Fig. 2), higher than the experiments of interest here. The precision of temperature characterization and the corresponding awkwardness in temperature adjustment is a practical limitation of these simulations that treat small systems over short times. Subsequent work should investigate temperature effects on these simulations, but we will proceed here in considering the results.

The structural analyses presented here, apply to the last 10 ps of the 18 ps trajectory. During this time, the initial structure with hydration number $n=19$ relaxed into structures with $n=15$ to $n=22$ neighbors within a radius of 5.1 Å (see Fig. 2). The resulting Kr–O radial distribution function, plotted with the solid line in Fig. 3, shows a build-up of water density to slightly more than double the bulk value, $g_{\max}(r) \approx 2.4$, at a radius $r \approx 3.7$ Å from the Kr atom. A comparison with the experimental XAFS data produced by Filipponi et al. [46] (Fig. 3) shows an overlap of error bars between the calculated and the experimentally determined radial distribution functions. The maximum value $g_{\max}(r) \approx 2.4$ is approximately the same as the value found from a force field model

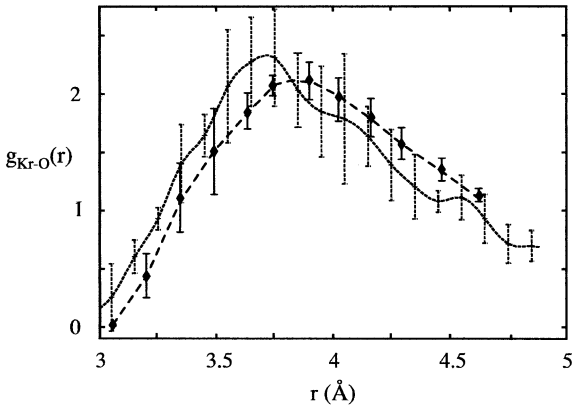

Fig. 3. Pair distribution function for Kr–O measured by experiment (dashed line) and by AIMD simulation (solid line). In the latter case, indicated error bars of $\pm 2\sigma$ were estimated on the assumption that the last four 2.5-ps trajectory segments are independent. Error bars of $\pm\sigma$ are plotted with the experimental data.

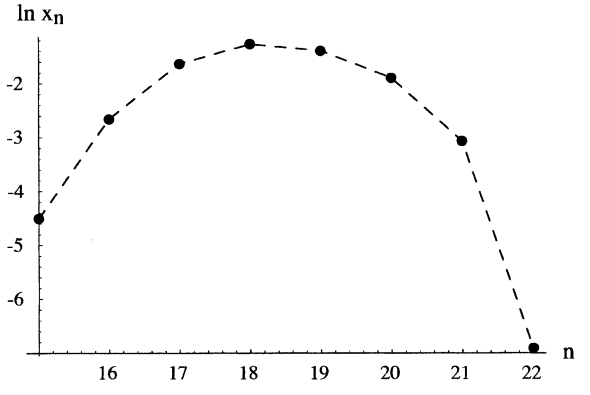

Fig. 4. Probability distributions of inner-shell structures with n water molecules surrounding the Kr atom where the inner-shell boundary is defined at $r=5.10$ Å.

adjusted to give experimental solution thermodynamics [11,12] and is slightly larger than the result found by Ashbaugh and Paulaitis [47] for the case of a corresponding sized hard sphere solute in SPC water, which is, as shown there, also in good agreement with the revised scaled particle model [48].

The average occupancy of the inner shell defined by the radius $r \leq 5.1$ Å is $\langle n \rangle = 18 \pm 1$ and $n=18$ is found also to be the most probable structure, as is shown in Fig. 4. The $n=20$ case is approximately half as likely as the most probable $n=18$ case, and either $n=19$ or $n=17$ is more probable than $n=20$ by these results. This x_n distribution of coordination numbers is unimodal. In a limited range of thermodynamic states approaching a clathrate phase boundary, the x_n distribution might be expected to exhibit magic number features reflecting metastable coordination possibilities [49]. Those possibilities are not observed here.

Consideration of the radial Kr–H pair distribution function (Fig. 5) shows a featureless distribution. These results are not dissimilar to recent computations of radial hydrogen distributions conditional on a hard sphere solute in SPC water [47]; although those calculations have better spatial resolution and thus additional observable structure, the maximum hydrogen density is approximately the same here.

Although these calculations have clear limitations of scale and thus correspondence to the experiment, to within the errors of the theoretical and experimental measurements, *they do corroborate the experimentally observed local fluid structure*. They provide also the more probable features of the coordination number distribution, x_n, of physical interest from the point of view of quasi-chemical models. The coordination structures observed in the AIMD simulation should provide an appropriate starting point in considering inner

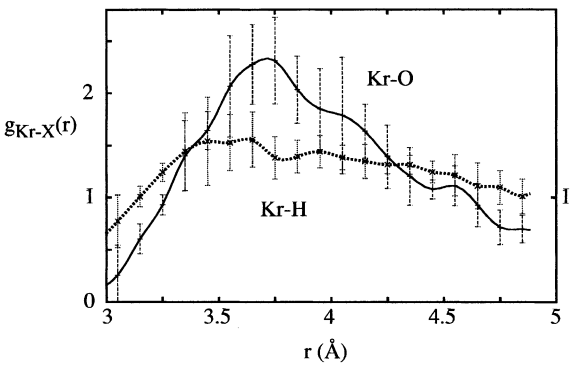

Fig. 5. Pair distribution function for Kr–O and Kr–H determined by AIMD simulation. Error bars indicate the estimated 95% confidence level.

shell coordination species that might found quasi-chemical models.

The following sections consider the outer and inner shell contributions to the hydration free energy of Kr in turn.

5. Outer shell contributions

The outer shell term would be the hydration free energy under the hypothetical constraint that inner shell occupancy be prohibited. We anticipate that an electrostatic contribution, estimated with a dielectric continuum model, will be included in the modified equilibrium ratios obtained below; see Eq. (4) and the supporting discussion. For the Kr case considered here, that leaves packing interactions associated with hard spherical exclusion volume and weaker London dispersion interactions. We will discuss those outer shell contributions here—scaled particle theory provides a connection between outer shell contributions to the free energy and the packing of water about an evacuated cavity. The free energy for emptying the inner sphere is given by the work of growing a hard sphere solute in aqueous solution

$$\beta\mu^{ex}(\text{outer shell}) = 4\pi\rho_{H_2O}\int_0^R G(\lambda)\lambda^2 d\lambda \qquad (5)$$

where R is the inner shell radius, and $G(\lambda)$ is the contact value of the cavity-water oxygen radial distribution function that depends on the distance of closest approach λ. This expression can be thought of as the $p\cdot dV$, $\rho_{H_2O}kTG(\lambda)\cdot 4\pi\lambda^2 d\lambda$, work associated with growing an empty cavity into solution. The surface tension associated with differentially increasing the surface area of the outer shell cavity is given by the derivative of Eq. (5) with respect to the outer shell surface area

$$\beta\gamma(R) = \left(\frac{\partial\beta\mu}{\partial R}\right)\frac{\partial R}{\partial(4\pi R^2)} = \frac{1}{2}\rho_{H_2O}G(R)R \qquad (6)$$

This derivative has also been approximated simply by the ratio of the hydration free energy of exclusion volume to its surface area

$$\beta\gamma(R) \approx \rho_{H_2O}\int_0^R G(\lambda)\left(\frac{\lambda}{R}\right)^2 d\lambda \qquad (7)$$

These two distinct expressions, Eqs. (6) and (7), yield different values for the surface tension for submacroscopic cavities.

The contact function $G(\lambda)$ is readily obtained from molecular simulations of hard sphere hydration at discrete values of λ. Alternatively, Stillinger proposed [48] a functional form for $G(\lambda)$ that interpolates between the known microscopic and macroscopic limiting forms:

$$G(\lambda) = \begin{cases} \dfrac{1+(\pi\rho/\lambda)\int_0^{2\lambda} g_{OO}(z)(z-2\lambda)z^2 dz}{1-4\pi\rho\lambda^3/3+(\pi\rho)^2\int_0^{2\lambda} g_{OO}(z)\left(z^3/6-2\lambda^2 z+8\lambda^3/3\right)z^2 dz}, & \lambda < 1.75\ \text{Å} \\ p_{sat}/\rho kT + \dfrac{(2\gamma l_v/\rho kT)}{\lambda} + \dfrac{G_2}{\lambda^2} + \dfrac{G_4}{\lambda^4}, & \lambda > 1.75\ \text{Å} \end{cases} \qquad (8)$$

where g_{OO} is the water oxygen–oxygen radial distribution function, p_{sat} is the saturation pressure of water in equilibrium with its vapor, and γ_{lv} is the vapor–liquid surface tension. The coefficients G_2 and G_4 are chosen so that the contact function is seamless, matching $G(\lambda)$ and its first derivative at $\lambda = 1.75$ Å, different from the originally suggested 1.95 Å [48,47]. Extensive molecular simulations [47] have verified Stillinger's functional form for water and give confidence for calculating outer shell contributions to the hydration of Kr.

To this end we have used simulation results for the radial distribution function of SPC/E water along the saturation line (Prof. S. Garde, personal communication) with the experimental surface tension of water and the corresponding surface hydration properties to evaluate $G(\lambda)$ using Eq. (8). The resulting surface tension as a function of cavity size at 25 °C is shown in Fig. 6. While Eqs. (6) and (7) for the surface tension are zero for a cavity of zero size and converge to the same ultimate value for an infinite cavity ($\gamma = 0.411$ kJ/mol·Å^2 = 72 dyn/cm) assuming the saturation pressure of water is negligible, they differ at intermediate molecular sizes. In particular, Eq. (6) nearly attains its plateau value for cavities on the order of 5–10 Å in radius, while Eq. (7) more

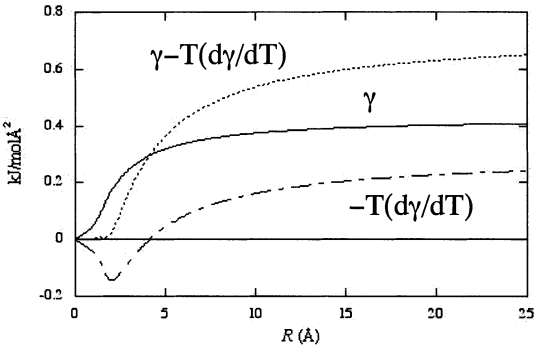

Fig. 6. Apparent surface tension γ, and its temperature dependence, predicted by the revised scaled particle model of Eq. (6) at 25 °C, as a function of inner shell cavity radius. Where the solid curve exceeds the dotted curve, entropic contributions increase the value of this apparent surface tension.

slowly approaches the large sphere limit and is still less than 0.4 kJ/mol·Å^2 for the largest sizes considered. Particularly interesting is the temperature dependence of the outer shell cavity hydration free energy; Fig. 6 shows a distinct negative entropy for hydrophobic hydration for molecularly sized cavities that dominates the hydration free energy and is consistent with the known thermodynamic characteristics of small hydrophobe hydration. With increasing cavity size the entropy changes sign and becomes favorable with increasing size, approaching the surface free energy of a flat surface. Drying phenomena are, of course, not a separate issue for this revised scaled particle model [4,50,51].

The formula in Eq. (5) gives a free energy contribution of 9 kcal/mol which represents the work of rearranging water to grow an empty cavity of radius $R=3.9$ Å corresponding approximately to the distance of the inner shell water molecules in minimum energy cage structures discussed below. The first-order perturbation theory estimate [52] of the effects of dispersion interactions between the Kr solute and outer shell water molecules is $-\frac{16\pi\epsilon}{3}\times\left(\frac{\sigma}{R_0}\right)^3\rho_W\sigma^3$; with $\epsilon=0.19$ kcal/mol, and $\sigma=3.38$ Å, the Lennard–Jones parameters for Kr–W van der Waals interactions, this is approximately -3 kcal/mol with $R_0=3.9$ Å.

We conclude this discussion by emphasizing the important point that this treatment of the outer shell term gives a positive contribution of approximately 6 kcal/mol. The experimental value for the hydration free energy of Kr(aq) is approximately 2 kcal/mol [53]. Although these observations are straight-forward, the non-trivial implication here is that the inner shell contribution must be *negative* and of comparable size.

6. Inner shell structures and contributions

The advantage of the quasi-chemical formulation is that Eq. (4) is a reasonable initial approximation to the equilibrium constants for complex formation in solution, the quantities sought for the inner shell contribution to the solute hydration free energy. The harmonic approximation to $K_m^{(0)}$ is available from electronic structure calculations.

Fig. 1 shows inner shell structures that have been obtained and we note some basic observations. Firstly, these complexes are large enough that satisfactory electronic structure calculations are non-trivial [54]. Secondly, finding mechanically stable structures for these complexes is non-trivial, particularly for values of $n<18$. For example, extracting inner shell structures from the AIMD trajectory and then energy optimizing always resulted in decomposition, i.e. some of the water molecules were repositioned to the outer shell and then $b(\mathbf{j})=0$ for some $\mathbf{j}$. Finding mechanically stable complexes required some subtlety, as described below, and still only $n\geq 18$ complexes were obtained.

A 20-vertex pentagonal dodecahedron cage, present as the small cavity in all known clathrate hydrate structures [17], was built enclosing a Kr atom in several steps. First we built a carbon cage and minimized that structure with molecular mechanics. Then each vertex of this dodecahedron was replaced by oxygen atoms and hydrogen atoms were added to give a cage composed of water molecules with the Kr embedded inside it. This structure was energy minimized with a molecular mechanics potential for Kr–water interactions. The minimization occurred over multiple stages in

which the force constant of a harmonic force restraining the oxygen atoms was progressively decreased. The final structure obtained with a low force constant (5 kcal/mol/Å^2) was then subjected to quantum chemical optimization. The $n=19$ and $n=18$ structures were obtained by removal of water molecules from the optimized $n=20$ structure. For the $n=18$ structure, we had to once again go through the routine of employing molecular mechanics before any cage-like structure could be obtained.

Limited computational resources permitted only optimizations using HF/6-31G theory. The quantum chemical optimizations first employed steepest descent to relax the molecular mechanics structure rapidly with the final geometry obtained using the Newton–Raphson procedure. All calculations were performed using Gaussian [55]. Frequencies (and zero-point and thermal contributions to the free energy) were computed at the HF/6-31G level of theory. Non-negative curvatures confirmed a true minimum. These structures (Fig. 1) are clearly metastable and the difficulty in finding these minima suggests that the catchment volumes are small.

For the single point energies we used the B3LYP hybrid density functional, but with two different basis sets. This functional does not account for Kr–H_2O interactions of London dispersion character; but it does treat electrostatic induction phenomena and is adequate for water–water interactions. We will address this omission of Kr–H_2O dispersion interactions later. The basis sets were 6-31+G(d,p) for all atoms or the 6-31G for Kr and a much larger 6-311+G(2d,p) basis for the O and H atoms. Only the results with the latter choice are presented here (see Table 1).

The electrostatic contributions required by Eq. (4) for the Kr$[H_2O]_n$ cluster and the individual water molecules were computed using a continuum dielectric model. The exterior of the system was assigned the dielectric constant of liquid water and the interior had a dielectric constant of 1. The calculations were performed using a boundary integral formulation of the governing equations [56], with the surface tessellation obtained using the MSMS program [57]. The partial atomic charges needed in this calculation were ESP charges obtained using the ChelpG procedure in Gaussian [55]. For the charge fitting procedure, the Gaussian default radii for O (1.75 Å) and H (1.45 Å) atoms were used. For Kr a radius of 2.0 Å was used. A radius of 3.0 Å for Kr leads to an unphysically high positive charge on the Kr atom and therefore was not used. The solvation free energies are, in fact, insensitive to this choice and the values differ by only approximately 0.6 kcal/mol. Table 1 summarizes the inner shell results.

Table 1
ΔE, electronic energy change upon complexation; ΔG_{corr}, zero-point and thermal corrections upon complexation; ΔG_{298} is the free energy change accounting for the actual density of water, that is the free energy change at 1 atm; pressure is adjusted by $-nRT\ln(1354)$; $\Delta\mu$ is the change in the solvation free energy; $\Delta G_{(aq)}$ is the excess chemical potential of Kr for the assumed hydration structures; and all values are in kcal/mol

n	ΔE	ΔG_{corr}	ΔG_{298}	$\Delta\mu$	$\Delta G_{(aq)}$
18	−195.6	220.6	−52.4	93.0	40.6
19	−204.2	226.6	−59.3	98.4	39.1
20	−218.9	245.9	−59.0	105.7	46.7

In the calculations above, the zero-point energies were scaled by a factor of 0.9135. This factor is suitable for the HF/6-3lG(d) level and has been used for the present HF/6-31G level calculations. For the cases that we could build closed cages, we included an approximate correction for residual entropy corresponding to conformational multiplicity. Assuming ideal tetrahedral coordination for each water, this residual entropy amounts to $S/k \approx \ln(3/2)^n$ [58], where n is the number of water molecules in the cage. Further, MP2 level calculations that do treat dispersion interactions between an isolated Kr–water pair suggest a correction that amounts to approximately −0.3 kcal/mol for each Kr–water pair; the excess chemical potentials would need to be adjusted by this amount also. Thus, for the $n=18$ case, the excess free energy of Kr is 30.9 kcal/mol and 35.9 kcal/mol for the $n=20$ case. With or without these additional corrections, it is clear that the inner shell contribution is in the range of 30–50 kcal/mol, which is an order of magnitude greater than the experimental value of approximately 2 kcal/mol. Note that accuracies of 2 kcal/mol are barely achievable with all but the highest level of electronic structure methods.

Considering the balance of inner and outer shell contributions, we return to the fact that the accurately known outer shell contributions discussed above are positive and larger than the thermodynamical value. This implies that the inner shell contributions must be negative and approximately as large in magnitude as the experimental value. Here, our estimates for that inner-shell contributions are positive and large; this qualitative situation is unlikely to change substantially with more sophisticated electronic structure calculations. We conclude that the effects of the medium external to our clusters are decisive in stabilizing these structures. They must help to pull open and stabilize the cage. This physical realization is consistent with Sloan's view that these structures should be visualized as *dandelions* rather than spherical complexes [17].

More specifically, the results of Table 1 suggest that the dielectric model used here to describe the influence of the outer sphere material, though satisfactory for some corresponding ion hydration problems, is not satisfactory for the present application. It is possible that the effective fields, hinted following Eq. (4), which are self-consistent with the known fluid densities and reflect the influence of outer shell material on the K_ns [38,51], should describe these effects more satisfactorily, but resolution of that possibility will remain for subsequent work.

7. 'What are we to tell students?'

Work on the problem of hydrophobic effects has the maturity of many decades of effort; that time scale certainly reflects the difficulty of this theoretical problem. A conceptualization reflecting that maturity might be subtle, expressing the complexity of water as a material, but can be simple. An example of a surprising simple result is the formula

$$\mu^{ex}_{\mathrm{Kr(aq)}} = -A\rho_W(T) + BT\rho_W(T)^2 + CT \qquad (9)$$

with parameters A, B and C, and $p_W(T)$ is the density of liquid water coexistence with its vapor at temperature T [4]. That this formula describes signature hydrophobic thermodynamic properties for small hydrophobic solutes was unanticipated [59], but it would have been unreasonable to hope for a simpler result. This simple formula points to the distinctive equation of state of liquid water as a primary feature of hydrophobicity.

A recent attempt at an answer to 'what are we to tell students' appeared in [5]. That attempt tried to produce a faithful physical paraphrase of the recent molecular theories which, though non-committal on simple structural hypotheses, have identified a simple explanation of entropy convergence of hydrophobicities [59–61]. Here, we refine and thus simplify that previous answer.

Several points can be made in preparation for this discussion. Firstly, we note that the revised scaled particle model [48] is the most successful theory of hydrophobicity for spherical solutes [47,62,63]. The widely recognized point that '…the orientational arrangement of vicinal water molecules, is absent from the theory' [64] does *not* mean that these theoretical approaches are specifically approximate because of a neglect of orientational effects. Though the truth-content of this assertion has never changed, reappreciation of molecular theories has made this point explicit over recent years [4,8,65]. In fact, the revised scaled particle model along with the Pratt–Chandler theory [66], the information theory models [8,34], and quasi-chemical treatments [4] specifically do not neglect orientational effects. What is more, because these theoretical models firmly incorporate experimental information [65], they do not assume that H-bonding among water molecules is non-cooperative, as is the case for most computer simulations of aqueous solutions.

Secondly, hydrophobicity as judged by hydration free energy is greatest at moderately elevated temperatures >100 °C along the vapor saturation curve, as was emphasized by [67]. This observation may be non-canonical [68–70]; but the unfavorable hydration free energy of simple hydrophobic species is an objective property of those systems and is largest in these higher temperature thermodynamic states. What is more, the most provoking puzzle for molecular mechanisms of hydrophobia phenomena has always been the apparent increase in attractive strength of hydrophobic effects with increasing temperature for temperatures not too high. This point is experi-

mentally clear in the phenomena of cold-denaturation wherein unfolded soluble proteins fold *upon heating*. [See for example, Li et al. [71]. Proteins *are* complex molecules, but in that elastin example no hydrophilic side chains complicated the considerations in that way. And the experimental temperature for collapse upon heating (27 °C) is in the stable range of the liquid phase of water.] This point is conceptually troublesome because the molecular structural pictures, including clathrate models, seem to point to low temperature regimes and behaviors as identifying the essence of hydrophobicity. The discussion of Stillinger [72], which suggested connections between the behaviors of supercooled liquid water and hydrophobic effects, provides an example of those intuitions.

There are two characteristics of liquid water that are featured in the new answer that we propose. The first characteristic is that the liquid water matrix is stiffer on a molecular scale than are comparative organic solvents when confronted with the excluded volume of hydrophobic molecular solutes [5,8,63,73]. An indication of this relative stiffness is provided by comparison of experimental compressibilities of the usual solvents [4]. We do not give a structural picture for that relative stiffness, but it is due to intermolecular interactions among solvent molecules, H-bonding in the case of liquid water [74]. This stiffness is the principal determinant of the low solubility of inert gases in liquid water. Furthermore, this stiffness is weakly temperature-dependent in the case of liquid water. This temperature insensitivity is again suggested by consideration of the isothermal compressibility of water; the temperature variation of that isothermal compressibility displays a minimum at 46 °C and low pressure. In theories such as Eq. (8), this stiffness and its temperature dependence is carried by the experimental $g_{OO}(r)$, which is distinctive of liquid water.

[We note in passing, that the liquid–vapor interracial tension and its temperature dependence, $\gamma_{lv}(T)$, appears also in the model of Eq. (8). In previous scaled particle models where this empirical information was not specified, the temperature dependence of the implied $\gamma_{lv}(T)$ was found to be improper [48,75], though the magnitude of this parameter in the temperature region of most interest was reasonable. In some other important aspects that more primitive scaled particle model was satisfactory [76,77]. Thus, a reasonable view is that the specific empirical temperature dependence of $\gamma_{lv}(T)$ better resolves the conflicting temperature dependencies, but is secondary to the classic hydrophobic temperature dependencies that are clearest for submacromolecular scales (see Fig. 6).]

The second characteristic in our answer is the variation of the liquid density along the liquid–vapor coexistence curve in the temperature regimes of interest here [61]. The critical temperature of liquid water is significantly higher than is the case for the comparative organic solvents. The coefficient of thermal expansion along the coexistence curve, α_σ [78], is typically more than five times smaller for water than for common organic solvents. It is a secondary curiosity that liquid water has a small regime of density increase with increasing temperature; we are interested here in a much broader temperature region. Nevertheless, the densities of typical organic solvents decrease more steadfastly with increasing temperature than does the density of water.

These two points lead to a picture in which the aqueous medium is stiffer over a substantial temperature range and expands with temperature less significantly than the natural comparative solvents. If these structural features of the aqueous medium are thus buffered against normal changes with increasing temperatures, then at higher temperatures the solvent exerts a higher kinetic pressure through repulsive collisions with hydrophobic solutes which do not experience other interactions of comparable significance. These collisions are proportionally more energetic with increasing temperature and the aqueous environment thus becomes more unfavorable for hydrophobic solutes with increasing temperature. The rate of density decrease with increasing temperature eventually does dominate this mechanism at the highest temperatures of interest here, >100 °C, and less unconventional behavior is then expected. This is our response to 'what are we to tell students?'

If a balancing act minimizing the variations of the structure of the aqueous medium with temperature is possible, it should be a useful trick since

it should have the consequence of expanding the temperature window over which biomolecular structures are stable and functional [5].

We emphasize again, as in Pratt and Pohorille [5], that hydrogen bonding, tetrahedrality of coordination, random networks and related concepts are not direct features of this answer. Nevertheless, they are relevant to understanding liquid water; they are elements in the bag of tricks that is used to achieve the engineering consequences that are discussed in the picture above.

8. Conclusions

The coordination number of Kr in liquid water solution is significantly different from known clathrate hydrate phases. These coordination numbers play a direct role in quasi-chemical descriptions of the hydration thermodynamics. Thus, the coordination number differences between liquid solution and clathrate phases can be expected to lead to substantial thermodynamic effects. In these respects, a clathrate picture is not supported by our current information on the molecular scale hydration of Kr(aq); the euphemism 'clathrate-like' has to be understood as 'clathrate-unlike' in these respects.

The present results for the distribution of Kr(aq) coordination numbers give no suggestion of lower probability, metastable, magic number coordination structures that might reflect the coordination possibilities in a known, lower temperature, clathrate hydrate phase; see Fig. 4.

The isolated inner shell Kr[H20]n complexes that have been obtained for $n=18$, 19 and 20 have a delicate stability. When inner shell coordination structures were extracted from the simulation of the liquid, and then subjected to quantum chemical optimization, they decomposed. Inner shell complexes for $n<18$ were not found here, and therefore possibilities for inner shell complexes that cover the coordination number range observed in the simulation were not found. Evidently, interactions with the outer shell material can be decisive in stabilizing coordination structures observed in liquid solution and in clathrate phases.

Although quasi-chemical approaches are formally exact and efficient in applications to the hard sphere fluid [38,51] and to ion hydration problems [39,40], these ab initio quasi-chemical theories applied to Kr(aq) will be more difficult. Several contributions have to be assembled that are an order-of-magnitude larger than the net result for the hydration free energy. Modest errors in any one of those several contributions can easily destroy any reasonable correspondence with experimental results.

We have developed a response to the 'what are we to tell students' question that is based upon the known thermodynamic peculiarities of liquid water and does not require specific molecular structural hypotheses. In addition to that simple argument, we can tell students several other points of context. We can tell students that although the primitive concepts of hydrophobic effects based upon water–oil fluid phase separation are reasonable, the structural molecular conceptualizations of hydrophobic effects, such as clathrate models, have achieved *no* consensus. A lack of specificity and quantitativeness in the thermodynamic analyses of these molecular pictures contributes to this lack of consensus. We can tell students that there is an orthodox clathrate picture that is not literally correct. A reformed 'clathrate-like' picture also appears in the extant literature; this reformed picture suggests connections to the orthodox picture, and could be regarded as a poetic 'explanation', borrowing Stillinger's identification of a limiting possibility. Established quantitative connections to signature thermodynamic properties are not available for either the orthodox or the reformed 'clathrate-like' pictures of hydrophobic hydration.

Despite the fact that the various molecular scale pictures have not been proven, a role for molecular theory in this setting can follow the conventional understanding of scientific inference: approximate theories should provide clear expression of a physical idea at a molecular level and should be quantitatively testable. The degree of success in those tests then contributes to the degree of confidence in the physical pictures. Molecular mechanisms that are tested only at an impressionistic level, even after an investment in quantitative computer simulations, are less conclusive.

This discussion leads to consideration of Ockham's razor [79]. For thermodynamics of primitive hydrophobic effects, we have simple, logical, well-tested molecular theories [4] and those theories do not explicitly involve structural mechanisms such as clathrate models. Additional hypotheses in response to 'what are we to tell students' are not required at this stage.

Acknowledgments

The work was supported by the US Department of Energy, contract W-7405-ENG-36, under the LDRD program at Los Alamos and Sandia, LA-UR-02-6362.

References

[1] W. Kauzmann, Some factors in the interpretation of protein denaturation, Adv. Protein Chem. 14 (1959) 1–63.
[2] C. Tanford, How protein chemists learned about the hydrophobia factor, Protein Science 6 (1997) 1358–1366.
[3] T. Lazaridis, Solvent size vs. cohesive energy as the origin of hydrophobicity, Ace. Chem. Res. 34 (2001) 931–937.
[4] L.R. Pratt, Molecular theory of hydrophobic effects: 'She is too mean to have her name repeated', Annu. Rev. Phys. Chem. 53 (2002) 409–436.
[5] L.R. Pratt, A. Pohorille, Hydrophobic effects and modeling of biophysical aqueous solution interfaces, Chem. Rev. 102 (2002) 2671–2691.
[6] D.T. Bowron, A. Filipponi, M.A. Roberts, J.L. Finney, Hydrophobic hydration and the formation of a clathrate hydrate, Phys. Rev. Letts. 81 (1998) 4164–4167.
[7] H.S. Frank, M.W. Evans, Free volume and entropy in condensed systems. III. Entropy in binary liquid mixtures; partial molar entropy in dilute solutions; structure and thermodynamics of aqueous electrolytes, J. Chem. Phys. 13 (1945) 507.
[8] G. Hummer, S. Garde, A.E. García, L.R. Pratt, New perspectives on hydrophobic effects, Chem. Phys. 258 (2000) 349–370.
[9] M.E. Paulaitis, L.R. Pratt, Hydration theory for molecular biophysics, Adv. Prot. Chem. (in press).
[10] S. Swaminathan, S.W. Harrison, D.L. Beveridge, Monte Carlo studies on structure of a dilute aqueous-solution of methane, J. Am. Chem. Soc. 100 (1978) 5705–5712.
[11] W.C. Swope, H.C. Andersen, A molecular-dynamics method for calculating the solubility of gases in liquids and the hydrophobia hydration of inert-gas atoms in aqueous-solution, J. Phys. Chem. 88 (1984) 6548–6556.
[12] K. Watanabe, H.C. Andersen, Molecular-dynamics study of the hydrophobic interaction in an aqueous-solution of krypton, J. Phys. Chem. 90 (1986) 795–802.
[13] D. Chandler, J.D. Weeks, H.C. Andersen, Van der Waals picture of liquids, solids, and phase-transformations, Science 220 (1983) 787–794.
[14] Y.A. Dyadin, E.G. Larionov, A.Y. Manakov, F.V. Zhurko, E.Y. Aladko, T.V. Mikina, V.Y. Komarov, Clathrate hydrates of hydrogen and neon, Mendeleev Comm. (1999) 209–210.
[15] V.I. Kosyakov, V.A. Shestakov, Simulation of phase equilibria in the water-helium and water-neon systems, Russ. J. Phys. Chem. 76 (2002) 716–719.
[16] W.L. Mao, H.-K. Mao, A.F. Goncharov, V.V. Struzhkin, Q. Guo, J. Hu, et al., Hydrogen clusters in clathrate hydrate, Science 297 (2002) 2247–2249.
[17] E.D. Sloan Jr., Clathrate Hydrates of Natural Gases, 2nd ed, Marcel Dekker, Inc, New York, 1998. Revised and expanded edition.
[18] D. Eisenberg, W. Kauzmann, The Structure and Properties of Water, Oxford University Press, New York, 1969.
[19] Y. Cheng, P.J. Rossky, Surface topography dependence of biomolecular hydrophobic hydration, Nature 392 (1998) 696–699.
[20] D.N. Glew, Aqueous solubility and the gas-hydrates. The methane–water system, J. Phys. Chem. 66 (1962) 605–609.
[21] K.A. Dill, Dominant forces in protein folding, Biochem. 29 (1990) 7133–7155.
[22] I.M. Klotz, Protein hydration and behavior, Science 128 (1958) 815–822.
[23] L. Pauling, The structure of water, in: D. Hadzi (Ed.), Hydrogen Bonding, Pergamon, New York, 1959, pp. 1–6.
[24] N.T. Southall, K.A. Dill, A.D.J. Haymet, A view of the hydrophobic effect, J. Phys. Chem. B 106 (2002) 521–533.
[25] T. Head-Gordon, Is water-structure around hydrophobic groups clathrate-like?, Proc. Nat. Acad. Sci. USA 92 (1995) 8308–8312.
[26] K.A. Udachin, J.A. Ripmeester, A complex clathrate hydrate structure showing bimodal guest hydration, Nature 397 (1999) 420–423.
[27] K.A. Udachin, C.I. Ratcliffe, J.A. Ripmeester, A dense and efficient clathrate hydrate structure with unusual cages, Angew. Chem. Int. Ed. 40 (2001) 1303.
[28] M.M. Teeter, Water-structure of a hydrophobic protein at atomic resolution: pentagon rings of water-molecules on crystals of crambin, Proc. Natl. Acad. Sci. USA 81 (1984) 6014–6018.
[29] L.A. Lipscomb, F.X. Zhou, L.D. Williams, Clathrate hydrates are poor models of biomolecule hydration, Biopolymers 38 (1996) 177–181.
[30] J.S. Tse, M.L. Klein, I.R. McDonald, Molecular-dynamics studies of ice Ic and the structure-I clathrate hydrate of methane, J. Phys. Chem. 87 (1983) 4198–4203.

[31] O.K. Forrisdahl, B. Kvamme, A.D.J. Haymet, Methane clathrate hydrates: melting, supercooling, and phase separation from molecular dynamics computer simulations, Mol. Phys. 89 (1996) 819–834.
[32] J.C. Owicki, H.A. Scheraga, Monte Carlo calculations in isothermal-isobaric ensemble. 2. dilute aqueous-solution of methane, J. Am. Chem. Soc. 99 (1977) 7413–7418.
[33] G. Alagona, A. Tani, Structure of a dilute aqueous-solution of argon: Monte–Carlo simulation, J. Chem. Phys. 72 (1980) 580–588.
[34] M.A. Gomez, L.R. Pratt, G. Hummer, S. Garde, Molecular realism in default models for information theories of hydrophobic effects, J. Phys. Chem. B 103 (1999) 3520–3523.
[35] H.L. Friedman, C.V. Krishnan, Water A Comprehensive Treatise, 3, Plenum Press, New York, 1973, pp. 1–118.
[36] L.R. Pratt, S.B. Rempe, Quasi-chemical theory and implicit solvent models for simulations, in: L.R. Pratt, G. Hummer (Eds.), Simulation and Theory of Electrostatic Interactions in Solution. Computational Chemistry, Biophysics, and Aqueous Solutions, AIP Conference Proceedings, 492, American Institute of Physics, Melville, NY, 1999, pp. 172–201.
[37] P. Grabowski, D. Riccardi, M.A. Gomez, D Asthagiri, L.R. Pratt, Quasi-chemical theory and the standard free energy of H^+(aq), J. Phys. Chem. A 106 (2002) 9145–9148.
[38] H.S. Ashbaugh, L.R. Pratt, A quasi-chemical self-consistent field model for the statistical thermodynamics of the hard sphere fluid, unpublished work.
[39] S.B. Rempe, L.R. Pratt, G. Hummer, J.D. Kress, R.L. Martin, A. Redondo, The hydration number of Li^+ in liquid water, J. Am. Chem. Soc. 122 (2000) 966–967.
[40] S.B. Rempe, L.R. Pratt, The hydration number of Na^+ in liquid water, Fluid Phase Equil 183 (2001) 121–132.
[41] Y. Wang, J.P. Perdew, Correlation hole of the spin-polarized electron gas with exact small-wave-vector and high-density scaling, Phys. Rev. B 44 (1991) 13298.
[42] G. Kresse, J. Hafner, Ab initio molecular-dynamics for liquid–metals, Phys. Rev. B 47 (1993) RC558.
[43] G. Kresse, J. Furthmüller, Efficient iterative schemes for ab initio total-energy calculations using a plane-wave basis set, Phys. Rev. B 54 (1996) 11169.
[44] D. Vanderbilt, Soft self-consistent pseudopotentials in a generalized eigenvalue formalism, Phys. Rev. B 41 (1990) 7892.
[45] G. Kresse, J. Hafner, Norm-conserving and ultrasoft pseudopotentials for first-row and transition-elements, J. Phys. Condens. Matter 6 (1994) 8245.
[46] A. Filipponi, D.T. Bowron, C. Lobban, J.L. Finney, Structural determination of the hydrophobic hydration shell of Kr, Phys. Rev. Lett. 79 (1997) 1293–1296.
[47] H.S. Ashbaugh, M.E. Paulaitis, Effect of solute size and solute–water attractive interactions on hydration water structure around hydrophobic solutes, J. Am. Chem. Soc. 123 (2001) 10721–10728.
[48] F.H. Stillinger, Structure in aqueous solutions of nonpolar solutes from the standpoint of scaled-particle theory, J. Sol. Chem. 2 (1973) 141–158.
[49] J.P. Long, E.D. Sloan Jr., Quantized water clusters around apolar molecules, Mol. Sim. 11 (1993) 145–161.
[50] K. Lum, D. Chandler, J.D. Weeks, Hydrophobicity at small and large length scales, J. Phys. Chem. B 103 (1999) 4570–4577.
[51] L.R. Pratt, R.A. LaViolette, M.A. Gomez, M.E. Gentile, Quasi-chemical theory for the statistical thermodynamics of the hard-sphere fluid, J. Phys. Chem. B 105 (2001) 11662–11668.
[52] M.P. Allen, D.J. Tildesley, Computer Simulation of Liquids, Oxford Science Publications, Oxford, 1987.
[53] H.L. Clever, Krpton, xenon, and radon-gas solubilities, in: H.L. Clever (Ed.), Solubility Data Series, 2, Pergamon Press, New York, 1979.
[54] R. Ludwig, F. Weinhold, Quantum cluster equilibrium theory of liquids: Freezing of QCE/3-21G water to tetrakaidecahedral 'Bucky-ice', J. Chem. Phys. 110 (1999) 508–515.
[55] M.J. Frisch, Gaussian 98 (Revision A.2), Gaussian, Inc, Pittsburgh, PA, 1998.
[56] B.J. Yoon, A.M. Lenhoff, A boundary element method for molecular electrostatics with electrolyte effects, J. Comp. Chem. 11 (1990) 1080–1086.
[57] M.F. Sanner, J.-C. Spehner, A.J. Olson, Reduced surface: an efficient way to compute molecular surfaces, Biopolymers 38 (1996) 305–320.
[58] L. Pauling, The structure and entropy of ice and of other crystals with some randomness of atomic arrangement, J. Am. Chem. Soc. 57 (1935) 2680–2684.
[59] S. Garde, G. Hummer, A.E. García, M.E. Paulaitis, L.R. Pratt, Origin of entropy convergence in hydrophobic hydration and protein folding, Phys. Rev. Lett. 77 (1996) 4966–4968.
[60] S. Garde, H.S. Ashbaugh, Temperature dependence of hydrophobic hydration and entropy convergence in an isotropic model of water, J. Chem. Phys. 115 (2001) 977–982.
[61] H.S. Ashbaugh, T.M. Truskett, P.G. Debenedetti, A simple molecular thermodynamic theory of hydrophobic hydration, J. Chem. Phys. 116 (7) (2002) 2907–2921.
[62] L.R. Pratt, A. Pohorille, Theory of hydrophobicity: transient cavities in molecular liquids, Proc. Natl. Acad. Sci. USA 89 (1992) 2995–2999.
[63] L.R. Pratt, A. Pohorille, Hydrophobic effects from cavity statistics, in: M.U. Palma, M.B. Palma-Vittorelli, F. Parak (Eds.), Proceedings of the EBSA 1992 International Workshop on Water–Biomolecule Interactions, Societá Italiana de Fisica, Bologna, 1993, pp. 261–268.
[64] B. Guillot, Y. Guissani, A computer simulation study of the temperature dependence of the hydrophobic hydration, J. Chem. Phys. 99 (1993) 8075–8094.
[65] L.R. Pratt, G. Hummer, S. Garde, Theories of hydrophobic effects and the description of free volume in

complex liquids, in: C. Caccamo, J.-P. Hansen, G. Stell (Eds.), New Approaches to Problems in Liquid State Theory, NATO Science Series, 529, Kluwer, Netherlands, 1999, pp. 407–420.
[66] L.R. Pratt, D. Chandler, Theory of the hydrophobic effect, J. Chem. Phys. 67 (1977) 3683–3704.
[67] K.P. Murphy, P.L. Privalov, S.J. Gill, Common features of protein unfolding and dissolution of hydrophobic compounds, Science 247 (1990) 559–561.
[68] K.A. Dill, The meaning of hydrophobicity, Science 250 (1990) 297–297.
[69] P.L. Privalov, S.J. Gill, K.P. Murphy, Reply to Dill, Science 250 (1990) 297–297.
[70] J. Herzfeld, Understanding hydrophobic behavior, Science 253 (1991) 88–88.
[71] B. Li, D.O.V. Alonso, V. Daggett, The molecular basis for the inverse temperature transition of elastin, J. Mol. Biol. 305 (2001) 581–592.
[72] F.H. Stillinger, Water revisited, Science 209 (1980) 451–457.
[73] G. Hummer, S. Garde, A.E. García, M.E. Paulaitis, L.R. Pratt, Hydrophobic effects on a molecular scale, J. Phys. Chem. B 102 (1998) 10469–10482.
[74] T. Head-Gordon, F.H. Stillinger, An orientational perturbation-theory for pure liquid water, J. Chem. Phys. 98 (1993) 3313–3327.
[75] A. Ben-Naim, H.L. Friedman, On the application of the scale particle theory of aqueous solutions of nonpolar gases, J. Phys. Chem 71 (1967) 448–449.
[76] R.A. Pierotti, The solubility of gases in liquids, J. Phys. Chem. 67 (1963) 1840–1845.
[77] R.A. Pierotti, A scaled particle theory of aqueous and nonaqueous solutions, Chem. Rev. 76 (1976) 717–726.
[78] J.S. Rowlinson, F.L. Swinton, Liquids and Liquid Mixtures, Butterworths, London, 1982.
[79] R. Hoffman, V.I. Minkin, B.K. Carpenter, Ockham's razor and chemistry, HYLE: Int. J. Phil. Chem. 3 (1997) 3–28.